Vibration Analysis and Control of Rotating Composite Shaft Using Active Magnetic Bearings

A THESIS SUBMITTED IN THE PARTIAL FULFILLMENT OF THE REQUIREMENTS FOR THE DEGREE OF

Master of Technology

In

Mechanical Engineering

[Specialization: Machine Design and Analysis]

By

DILSHAD AHMAD

212ME1270

Department Of Mechanical Engineering
National Institute of Technology Rourkela
Rourkela, Orissa, India – 769008
June, 2014

Vibration Analysis and Control of Rotating Composite Shaft Using Active Magnetic Bearings

A THESIS SUBMITTED IN THE PARTIAL FULFILLMENT OF THE REQUIREMENTS FOR THE DEGREE OF

Master of Technology

In

Mechanical Engineering

[Specialization: Machine Design and Analysis]

By

DILSHAD AHMAD

212ME1270

Under The Supervision Of

Prof. T. Roy

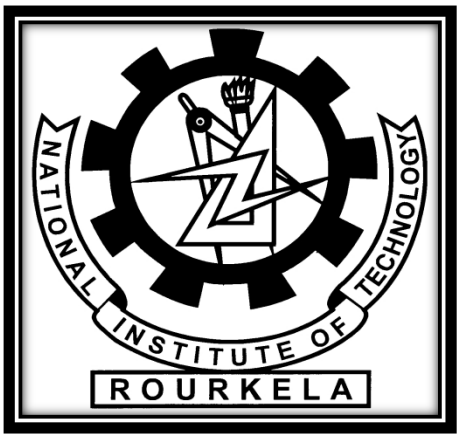

Department Of Mechanical Engineering
National Institute of Technology Rourkela
Rourkela, Orissa, India – 769008
June, 2014

DECLARATION

I hereby declare that this submission is my own work and that, to the best of my knowledge and belief, it contains no material previously published or written by another person nor material which to a substantial extent has been accepted for the award of any other degree or diploma of the university or other institute of higher learning, except where due acknowledgement has been made in the text.

(Dilshad Ahmad)

Date: 02-06-2014

NATIONAL INSTITUTE OF TECHNOLOGY ROURKELA

CERTIFICATE

This is to certify that the thesis entitled, ***"Vibration Analysis And Control Of Rotating Composite Shaft System Using Active Magnetic Bearings"*** *being submitted by* ***Mr. DILSHAD AHMAD*** *in partial fulfillment of the requirements for the award of* ***"MASTER OF TECHNOLOGY"*** *Degree in* ***"MECHANICAL ENGINEERING"*** *with specialization in* ***"MACHINE DESIGN AND ANALYSIS"*** *at the National Institute Of Technology Rourkela (India) is an authentic Work carried out by him under my supervision.*

To the best of our knowledge, the results embodied in the thesis have not been submitted to any other University or Institute for the award of any Degree or Diploma.

Date:

Dr. TARAPADA ROY
Department of Mechanical Engineering
National Institute of Technology
Rourkela-769008

ACKNOWLEDGEMENT

First and foremost I offer my sincerest gratitude and respect to my supervisor and guide *Dr. TARAPADA ROY*, Department of Mechanical Engineering, for his invaluable guidance and suggestions to me during my study. I consider myself extremely fortunate to have had the opportunity of associating myself with him for one year. This thesis was made possible by his patience and persistence.

After the completion of this Thesis, I experience a feeling of achievement and satisfaction. Looking into the past I realize how impossible it was for me to succeed on my own. I wish to express my deep gratitude to all those who extended their helping hands towards me in various ways during my tenure at NIT Rourkela. I greatly appreciate & convey my heartfelt thanks to my colleagues 'flow of ideas, dear ones & all those who helped me in the completion of this work. I am especially indebted to my parents and elder brother Dr. Khursheed Ahmad for their love, sacrifice, and support. They stood by me in all ups and downs of my life and have set great examples for me about how to live, study and work.

I also express my sincere gratitude to Prof. (Dr.) K. P. Maity, Head of the Department; Mechanical Engineering for valuable departmental facilities.

DILSHAD AHMAD

Roll No: - 212me1270

Index

Nomenclature

E	Young's modulus .
ν	Poisson's ratio.
ρ	Density.
v_0, w_0	Flexural displacements of the shaft axis.
β_x, β_y	Rotation angles of the cross-section about the *y* and *z* axis.
k_s	Shear correction factor.
$\overline{C}_{ijr}$	Constitutive matrix which is related to elastic constants of principle axes.
Ω	Rotating speed of the shaft.
L	Total length of the shaft.
I_m, I_d, I_p	Mass moment of inertia, diametrical mass moments of inertia and polar mass moment of inertia of rotating shaft per unit length respectively.
$I_{mi}^D, I_{di}^D, I_{pi}^D$	Mass moment of inertia, diametrical mass moment of inertia and polar mass moment of inertia of disks respectively.
$[M]$	Elemental mass matrix.
$[G]$	Elemental gyroscopic matrix.
$[C]$	Total elemental damping matrix.
$[K]$	Element structural stiffness matrix.
$\{F\}$	Elemental external force vector.
$\{q\}$	Elemental nodal displacement vector.

$[K_{Cir}]$ Skew-symmetric circulation matrix.

$[2\alpha]$ Included angle of the active magnetic bearing.

$[M_r]$ Rotational mass of the rotor.

$[i_0]$ Bias current.

$[i_{CY}, i_{CZ}]$ Control current in y and z direction respectively.

$[I_1, I_2]$ Main current in y and z direction respectively.

$[K_P]$ Position stiffness of active magnetic bearing either in y or z direction.

$[K_I]$ Current stiffness of active magnetic bearing either in y or z direction.

$[\omega]$ Rotational speed of the rotor.

List of Tables

List of Figures

ABSTRACT

The main aim of the project is to utilize the active vibration control technique to reduce vibration in composite shaft system using three nodded beam element. The fiber reinforced polymer (FRP) composite shaft is studied in this paper considering it as a Timoshenko beam. Three different isotropic rigid disks are mounted on it and also supported by two active magnetic bearings at its ends. The work involves finite element, vibrational and rotor dynamic analysis of the system. Rotary inertia effect, gyroscopic effect kinetic energy and strain energy of the shaft are derived and studied. The governing equation is obtained by applying Hamilton's principle using finite element method in which four degrees of freedom at each node is considered. Active control scheme is applied through magnetic bearings by using a controller containing low pass filter, notch filter, sensor and amplifier which controls the current and correspondingly control the stability of the whole rotor-shaft system. Campbell diagram, stability limit speed diagram and logarithmic decrement diagram are studied to establish the system stability. Effect of different types of stacking sequences are also studied and compared.

CHAPTER-1

INTRODUCTION

Vibration needs to be reduced in most of the rotor-shaft system so that an efficient functioning of the rotating machines is attained. Almost all rotating parts should be vibration free as it causes a lot of problems leading to instability of the system. Therefore there is a necessity to reduce the vibration level in rotating bodies for proper functioning of the system and different researchers are aiming for this. In the present days, composite materials are widely used for the manufacturing of rotor .It is because composites have light weight, high strength, high damping capacity. Weight of the composite materials is less because long stiff fibers are embedded in very soft matrix. Composites are made by at least two materials at macroscopic level. This type of unique reinforcement gives a lot of advantage for different applications. Fiber reinforced polymer (FRP) composite is a polymer matrix in which the reinforcement is fiber. The reinforcement of fiber can be done either by continuous fiber or by discontinuous fiber.

Active materials like piezoelectric material, magneto-strictive material, electromagnetic actuator and micro fiber carbon are also used for the vibration control of rotating parts. Piezoelectric material property to develop charge when mechanically stressed is utilized to bring control of vibration in moving parts. It is used as actuator as well as sensor in the system. Magnetostictive materials are like ferromagnetic material. Materials like cobalt, nickel and iron are magnetostictive materials and therefore change in the shape and size occurs when they are magnetized. Electromagnetic actuator is used very often as it gains the magnetic property when its coils are supplied with current and the displaced position of the rotor can be adjusted according to the current supply.

1.1 COMPOSITE MATERIALS

When two materials having different properties are combined together at macroscopic level, it results into a composite material. The mechanical properties of the composite materials are totally different from their constituent materials and also results in a superior one. Both materials are differing in their chemical composition and its properties. The resulting composite material is high in strength and other mechanical properties. Two types of composite materials are given as

- Particulate Composite
- Fibre Reinforced Composite

When particles of different sizes and shapes are mixed in a random way with the matrix, Particulate composites are formed. Mika flakes reinforced with glass, aluminum particles in polyurethane rubber are some examples of Particulate Composites.

Fibre reinforced composite material consist of fibres of significant strength and stiffness embedded in a matrix. Both fibres and matrix maintain their physical and chemical properties. Fibre reinforced composite having continuous fibres are more efficient. FRP can be classified into four categories according to matrix used such as: polymer matrix composites, metal matrix composites, ceramic matrix composite and carbon/carbon composites.

1.2 Lamina and Laminates

Lamina is also called ply and it shows one layer of composite material. This is the fundamental block of the composite materials. Unidirectional fibre reinforced materials show good properties like high strength and modulus but particularly in the direction of the fibres. On the other hand the properties are very poor in the direction other than the direction transverse to the fibres. Bonding between fibre and matrix is also important because a good bonding results in

higher strength of the composite structure. Discontinuous laminates have poor mechanical properties than continuous laminates.

Laminate is simply a collection of different laminas or ply. It is done to achieve desired stiffness and mechanical properties of the materials. The sequence of orientation of different ply in a single composite material is termed as stacking sequence. The layers are bonded with the same matrix material as that in a lamina.

Different types of laminates are classified as follows

- Symmetric Laminate
- Asymmetric Laminate
- Balanced Laminate
- Quasi isotropic Laminate

1.3 Vibration of Composite Shaft

When a body goes to and fro motion with respect to its equilibrium position, it is said to be vibrating. Vibration is an important phenomenon in engineering and should be checked in order to regain stability. Vibration can be classified as

- Free Vibration
- Forced Vibration
- Damped Vibration

When a body is vibrating without any aid of external agency, it is termed as free vibration. For example, if a spring- mass system is giving an external force initially and allowed to vibrate, it gradually comes to equilibrium position after some vibration. This is an ideal case of free vibration.

On the other hand if the same system is allowed to vibrate in to and fro motion and a constant external force is applied regularly to keep the system in vibration, it is said to be forced vibration.

Again if a damper like dashpot is used in the system in addition to spring, it makes the system to slow down its vibration gradually as dashpot provides friction. The use of damper in this way results in a damped vibration.

1.4 Active Vibration Control Techniques

When the vibration of rotor exceeds its limit, there is a great need to check its vibration and bring the system stability. Active control techniques are widely used for this purpose. It has a lot of advantages over other methods like better control quick action and compact view.

Some of the active vibration control can be classified as follows

- PD Control Action
- LQR Control Action
- PID Control Action
- Proportional Control Action
- Derivative Control Action

Proportional and derivative controllers are used in the PD control technique. The stability and overshoot problems that arise when a proportional controller is used at high gain can be achieved by adding a term proportional to the time-derivative of the error signal.

We need to operate a dynamical system at a very minimal cost. The case where the system dynamics are described by a set of differential equations which are linear and a quadratic function is used to describe the cost then it is called the LQ problem. The solution is obtained by the Linear Quadratic Regulator (LQR) which is a feedback controller.

CHPTER-2

LITERATURE REVIEW

2.1 Vibration Analysis and FE modeling of Composite Shaft System

Formulation for the rotor dynamic analysis of composite shaft system is done by considering the classical EMBT theory. Eight number of coefficient bearing is considered. Virtual work principle is applied to get the complete formulation. It emphasizes that the difference between EMBT and LBT theory is not so large [1]. A tapered composite Timoshenko shaft rotating with constant speed is studied. Galerkin method is applied for getting the solution of the equation. The effect of high speed is taken into consideration and compared with uniform steel shaft. It is found that by tapering, bending natural frequencies and stiffness can be significantly increased over those of uniform shafts having the same volume and made of the same material [2]. A composite shaft spinning axially is taken into consideration by Chang. M.Y [3]. The shaft is considered to carry three different isotropic rigid type disks and is supported by two bearings at its end. Bearings are modeled by viscous dampers and spring. Governing equation is found by applying Hamilton's principle. All effects like gyroscopic, shear deformation, coupling and rotary inertia are incorporated. Ghoneam.S.M [4] has studied the behavior of dynamic analysis of rotating shaft made of composite materials. The Campbell diagram is found out to compare the critical speeds for different laminate structure. Different parameters like stacking sequence, stability limit speed and volume fractions are well studied and compared. Boukhalfa.A [5] studied the spinning laminated composite shaft by taking a new method called h-p version of the finite element method. Dynamic behavior mainly eigen frequency changes with the change in the stacking sequences, ply angles, length, mean diameter

and thickness. He also established the fact that the critical speed of the spinning composite shaft is independent of the mean diameter and thickness ratio of the shaft. Jacquet-Richardet.G [6] dealt the dynamical analysis of rotating composite shaft with internal damping. A homogenized beam theory is considered for the formulation of symmetrical stacking sequence. For this purpose an experimental set up is carried out and used for validation. All the effect like stress stiffness, spin softening and internal damping are studied and postponed the instability limit. Chang.M.Y [7] analyzed that the composite shaft contains discrete isotropic rigid disks and is supported by bearings that are modeled as springs and viscous dampers. Based on a first-order shear deformable beam theory, the strain energy of the shaft are found by adopting the three-dimensional constitutive relations of material with the help of the coordinates transformation, while the kinetic energy of the shaft system is obtained via utilizing the moving rotating coordinate systems adhered to the cross-sections of shaft. Nelson.F.C [8] wrote a different type of thesis to understand the physical significance of rotordynamics. Natural critical speed, whirling speed, instability effects etc. and their physical effects are elaborated.

Shafts made up of different composite materials are widely used for this purpose due to its high stiffness and strength/weight ratio properties. Light weight Graphite/Epoxy material based shaft is used to study the lateral stability when running at high speed [9]. The dynamic behavior of composite shafts with particular interest on estimation of damping is studied [10]. This study analyzed the dynamic behavior of different materials such as glass/epoxy, carbon/epoxy, and boron/epoxy at different speeds. The stability behavior of a rotating composite shaft subjected to axial compressive loads is analyzed [11]. The critical speed of the thin-walled composite shaft is dependent on the stacking sequences, the length-radius ratio and the boundary conditions. The vibration behaviors of the rotating composite shafts containing

randomly oriented reinforcements are then studied [12]. Based on this model, the natural frequencies of the stationary shafts, and the whirling speeds as well as the critical speeds of the rotating shafts are investigated. The results reveal that the content and the orientation of reinforcements have great effect on the dynamic characteristics of the composite shafts. The dynamic stiffness matrix of a spinning composite beam is developed and then used to investigate its free vibration characteristics [13]. Of particular interest in this study is the inclusion of the bending–torsion coupling effect that arises from the ply orientation and stacking sequence in laminated fibrous composites.

Different configurations are studied for different number of plies and orientation angle and finds that for optimal configuration the natural frequency is increased up to a greater extent. A dynamical model is developed for the rotating composite shaft with shape-memory alloy (SMA) wires embedded in it [14]. SMA wires activation can significantly postpone the occurrence of the whirling instability and increase the critical rotating speed. Active composite material containing piezoelectric fiber is able to reduce transverse vibration of the shaft [15]. There is a noticeable increase in the natural frequency of the composite shaft due to activation of SMA wires [16]. The use of nitinol [shape memory alloy (SMA)] wires in the fiber-reinforced composite shaft, for the purpose of modifying shaft stiffness properties to avoid failures, is discussed.

2.2 Active Vibration Control Techniques in Rotor Shaft System

Many researchers have adopted different techniques of active controlling the vibration of rotating shaft in the past.

Schweitzer et al. et al. [17-18] developed an active way of bearing action and vibration control over an air gap which is more elegant. That measures the unbalance force with the help of sensor and applies the control force between the outer race and the bearing housing.

Schittenhelm et al [19] developed a linear quadratic regulator for a rotor system on the basis of a finite element model. The rotor is subjected to gyroscopic effect and is actively supported by means of piezoelectric actuators installed at one of its two bearings. Its dynamic behavior varies with the rotational frequency of the rotor. This aspect is challenging for linear time invariant control techniques since it results in a demand for high robustness. In this article a proposal for combined Linear Quadratic Regulator and Kalman Filter design on the basis of physical considerations is given.

Lund J. [20] categorized vibrations into two types, active and passive vibration and both passive and active means of vibration minimization techniques are elaborated. A suitable stiffness-damping combination is trying to get for the support to avoid or minimize resonant response. The passive category includes the use of flexible–damped supports, Squeeze-film dampers and viscoelastic bearing supports.

Allaire et al. [21] presented magnetic bearings in a multi mass rotor both as support bearings and vibration controller and shows the advantage of reducing amplitude of vibration by using an electromagnet. Two approaches is been used to actively control flexible rotors. In the first approach magnetic bearings or electromagnetic actuators are used to apply control forces directly to the rotor without making contact. In the second approach, the control forces of the electro-magnetic actuators are applied to the bearing housings.

Koroishi E. H. et al. [22] proposed a simple model of an electromagnetic actuator (EMA) for active vibration control (AVC) of rotor-shaft systems. The actuator used was linearized by

adopting a behaviour that is similar to the one used for active magnetic bearings (AMB). The results show the validity of the proposed model and the effectiveness of the control.

In recent years, Koroishi [23] developed a number of new methods to control acoustic and vibration attenuation. These have been developed aiming at handling different types of engineering problems related to the dynamic behaviour of the system. This is due to the demand for better and safer operation of mechanical systems. EMA uses electromagnetic forces to support the rotor without mechanical contact.

Keith et al. [24] analyzed that the use of electromagnetic bearings has been increased because it lowers the amplitude level.Also discussed that they generate no mechanical loss and need no lubricants such as oil or air as they support the rotor without physical contact.

Cheung et al. [25] presented the electromagnets to be open loop and unstable and all designs require external electronic control to regulate the forces acting on the bearing.

Abduljabbar et al. [26] developed an optimal controller based on characteristics peculiar to rotor bearing systems which takes into account the requirements for the free vibration and the persistent unbalance excitations. The controller uses feedback signals, the states and the unbalance forces. An approach of selecting the gains on the feedback signals has been presented based on separation of the signal effects. The results demonstrate that the proposed controller can significantly improve the dynamic behaviour of the rotor-bearing systems as far as resonance and instabilities are concerned. A passive vibration control devices are of limited use. This limitation together with the aim to exercise greater control over rotor vibration, with greatly enhanced performance, has led to a growing interest in the development of active control of rotor vibrations.

ROY T. et al [27] analysed that the linear quadratic regulator (LQR) control approach is effective in vibration control with appropriate weighting matrices, which gives different optimal control gain by minimizing the performance index. The weighting matrices [Q] and [R] are the most important components in LQR optimization. The combinations of [Q] and [R] matrices significantly affect the performance and input cost of the system and hence an optimal selection of these weighting matrices is of significant attention from the control point of view.

Serdar Cole M.O.T. et al [28] gave an idea to use the Active Magnetic Bearing (AMB) to attenuate the lateral vibration of a rotor under simultaneous excitations from mass unbalance and initial base impact, which is quasi-stationary in nature. For the implementation and testing of the devised multi frequency vibration control strategy, a flexible rotor facility was used. Multi frequency feedback control was applied in order to control vibration at the synchronous frequency and the first two harmonics.

Jingjun Zhang et al. [29] analysed that the transfer function is transformed to a state space vector dynamic equation for state feedback control system design. Linear Quadratic Regulator (LQR) based on independent mode space control techniques is designed to minimize the displacement of the system. The control voltage for the actuators is determined by the optimal control solution of the Linear Quadratic Regulator (LQR), which is very effectively used linear control technique. The recent years have seen the appearance of different new systems for acoustic and vibration attenuation, most of actuators then adding new actuator technologies. In this way, the study of algorithms for active vibrations control in rotating machinery has become a field of utmost interest, mainly due to the innumerable demands of an optimal performance of mechanical systems in aircraft automotive structures. Also, many critical machines such as

compressors, pumps and gas turbines continue to be used beyond their expected service life despite the associated potential for failure due to damage accumulation.

Koroishi, et al. [30] proposed that the AMB is a feedback mechanism that supports a spinning shaft by levitating it in a magnetic field. For this the sensor measured the shaft's relative position and correspondingly sends the signal to the controller. Then, the signal is amplified and fed as electric current to the magnet which generates an electromagnetic field that keeps the shaft in a desired position. The strength of the magnetic field depends both on the air gap between the shaft and the magnet and the dynamics of the system including the design.

Janik et al. [31] analysed that in order to invoke control force for reducing the amplitude of rotor vibration an electromagnetic actuator is used which is capable of applying non-contact type force of actuation over an air-gap. The actuator consists of four exciters (each having a pair of electromagnetic poles) arranged symmetrically within a stator casing around the periphery of the rotor. The advantage is that it can be placed at any suitable location along the span of the rotor-shaft avoiding the bearing as well as disc locations.

Dutt and Toi [32] considered a Polymeric material in the form of sectors as support bearing. Both stiffness and loss factor of such materials varies with the excitation frequency . Stiffness and loss factor have been found out for the support system comprising of polymeric sectors.

Meirovitch, L. [33] presented a mathematical and numerically verified modelling using the feedback pole allocation control. The aim of linear feedback control is to put the closed loop poles on the left half of the complex plane of the Eigen values, so as to ensure asymptotic stability of the closed loop system. Second approach consists of prescribing first the closed-loop poles associated with the modes to be controlled and then further computing the control gains

required to produce these poles. This particular approach is known as modal control because here the system is controlled by controlling its modes.

Clements J.R studied the active magnetic bearing and the research was to design, build and test a test rig that has the ability to excite an AMB system with large amplitude base excitation. Results obtained from this test rig will be compared to predictions obtained from linear models commonly used for AMB analysis and determine the limits of these models.

2.3 Motivation and Objective of Present Work

After going through all the related literatures of rotor shaft system, it is been seen that a lot of work related to mathematical modelling of the rotor shaft has been done. Finite element based modelling of different types of rotor shaft system has been completed. But as far as composite shaft system is concerned, a little work has been done. The use of the FRP composite materials for the rotor shaft is very advantageous due to its high strength to weight ratio, high stiffness to weight ratio, high durability and availability of different types of design flexibilities. Due to these properties the use of FRP composites in different operations provides less vibration and very suitable at higher rotational speed operations. To further control the vibration active control techniques are an important research topic.

Now the present work is an attempt to reduce the vibration of a FRP rotor-shaft system using PID control technique in Active Magnetic Bearing. The stability limit speed has been increased up to a good extent by applying control forces through proportional, derivative and integral control law which is fed by proximity pick-ups. It is seen that by using this method the additional stiffness and damping is added to the system which reduces unbalance response amplitude, exceeds critical speed limits and increases stability limit speed of the FRP rotor-shaft system. Finite element based vibration analysis of FRP composite shaft system is done with

disks and active magnetic bearings considering viscous and hysteresis damping. Mathematical modelling of Active magnetic bearing is also done. Ply angle effects are taken into account to study the vibrational stability of the whole system.

CHAPTER-3

MATHEMATICAL FORMULATION FOR FRP ROTOR SHAFT SYSTEM

3.1 Mathematical Modelling of FRP Composite Shaft

The shaft is modelled as a Timoshenko beam considering both rotary inertia and gyroscopic effect. The shaft is rotating at a constant angular speed along the longitudinal axis and has uniform circular cross section along the length. The displacement field is described by assuming the coordinate axis coincides with the shaft axis. The strain energy equation of the composite shaft can be derived by assuming the displacement fields as follows,

$$\begin{aligned} u_x(x,\ y,\ z,\ t) &= u(x,t)+z\beta_x(x,t)-y\beta_y(x,t) \\ u_y(x,\ y,\ z,\ t) &= v(x,t)-z\phi(x,t) \\ u_z(x,\ y,\ z,\ t) &= w(x,t)+y\phi(x,t) \end{aligned} \tag{1}$$

The stress-strain relationship considering cylindrical coordinate system is

$$\begin{bmatrix} \varepsilon_{xx} \\ \gamma_{x\theta} \\ \gamma_{xr} \end{bmatrix} = \begin{bmatrix} 0 & 0 & r\sin\theta\dfrac{\partial}{\partial x} & -r\cos\theta\dfrac{\partial}{\partial x} \\ -\sin\theta\dfrac{\partial}{\partial x} & \cos\theta\dfrac{\partial}{\partial x} & \cos\theta & \sin\theta \\ \cos\theta\dfrac{\partial}{\partial x} & \sin\theta\dfrac{\partial}{\partial x} & \sin\theta & -\cos\theta \end{bmatrix} \begin{bmatrix} v_0 \\ w_0 \\ \beta_x \\ \beta_y \end{bmatrix} \left(\frac{\pi}{2}-\theta\right) \tag{2}$$

The stress-strain relations for the r^{th} layer can be expressed in the cylindrical coordinate system as

$$\begin{bmatrix}\sigma_{xx}\\ \tau_{x\theta}\\ \tau_{xr}\end{bmatrix}=\begin{bmatrix}\overline{C}_{11\mathrm{r}} & k_s\overline{C}_{16\mathrm{r}} & 0\\ k_s\overline{C}_{16\mathrm{r}} & k_s\overline{C}_{66\mathrm{r}} & 0\\ 0 & 0 & k_s\overline{C}_{55\mathrm{r}}\end{bmatrix}\begin{bmatrix}\varepsilon_{xx}\\ \gamma_{x\theta}\\ \gamma_{xr}\end{bmatrix} \tag{3}$$

3.2 Strain Energy Expression for Composite Shaft

The strain energy equation of FRP composite shaft can be obtained as

$$U_s=\frac{1}{2}\int_V[\sigma]^T[\varepsilon]dV=\frac{1}{2}\int_V(\sigma_{xx}\varepsilon_{xx}+2\tau_{xr}\varepsilon_{xr}+2\tau_{x\theta}\varepsilon_{x\theta})dV \tag{4}$$

After simplification and taking first variation of above strain energy expression can be written as,

$$\delta U_S=\begin{bmatrix}B_{11}\begin{bmatrix}\int_0^L\left(\frac{\partial\beta_x}{\partial x}\frac{\partial\delta\beta_x}{\partial x}\right)dx\\ +\int_0^L\left(\frac{\partial\beta_y}{\partial x}\frac{\partial\delta\beta_y}{\partial x}\right)dx\end{bmatrix}+\frac{1}{2}k_sA_{16}\begin{bmatrix}\int_0^L\left(\beta_y\frac{\partial\delta\beta_x}{\partial x}+\frac{\partial\beta_x}{\partial x}\delta\beta_y\right)dx-\int_0^L\left(\beta_x\frac{\partial\delta\beta_y}{\partial x}+\frac{\partial\beta_y}{\partial x}\delta\beta_x\right)dx\\ -\int_0^L\left(\frac{\partial v_0}{\partial x}\frac{\partial\delta\beta_x}{\partial x}+\frac{\partial\beta_x}{\partial x}\frac{\partial\delta v_0}{\partial x}\right)dx-\int_0^L\left(\frac{\partial w_0}{\partial x}\frac{\partial\delta\beta_y}{\partial x}+\frac{\partial\beta_y}{\partial x}\frac{\partial\delta w_0}{\partial x}\right)dx\end{bmatrix}\\ +k_s(A_{55}+A_{66})\begin{bmatrix}\int_0^L\beta_x\delta\beta_x dx+\int_0^L\beta_y\delta\beta_y dx+\int_0^L\left(\frac{\partial v_0}{\partial x}\frac{\partial\delta v_0}{\partial x}\right)dx\\ +\int_0^L\left(\frac{\partial w_0}{\partial x}\frac{\partial\delta w_0}{\partial x}\right)dx-\int_0^L\left(\beta_y\frac{\partial\delta v_0}{\partial x}+\frac{\partial v_0}{\partial x}\delta\beta_y\right)dx+\int_0^L\left(\beta_x\frac{\partial\delta w_0}{\partial x}+\frac{\partial w_0}{\partial x}\delta\beta_x\right)dx\end{bmatrix}\end{bmatrix} \tag{5}$$

The terms of $A_{55}, A_{66}, A_{16}, B_{11}$ are given in the Appendix.

3.3 Kinetic Energy Expression for Composite Shaft

Kinetic energy expression and the first variation of the kinetic energy of FRP composite shaft can be obtained as follows,

$$\int_0^L\left[\mathrm{I_m}\left(\dot{v}_0^{\,2}+\dot{w}_0^{\,2}\right)+I_d\left(\dot{\beta}_x^{\,2}+\dot{\beta}_y^{\,2}\right)+\Omega^2I_p-2\Omega I_p\beta_x\dot{\beta}_y^{\,2}+\Omega^2I_d\left(\beta_x^{\,2}+\beta_y^{\,2}\right)\right]dx \tag{11}$$

$$T_s=\int_0^L\left[\mathrm{I_m}\left(\dot{v}_0\frac{\partial\delta v_0}{\partial t}+\dot{w}_0\frac{\partial\delta w_0}{\partial t}\right)+I_d\left(\dot{\beta}_x\frac{\partial\delta\beta_x}{\partial t}+\dot{\beta}_y\frac{\partial\delta\beta_y}{\partial t}\right)-\Omega I_p\left(\dot{\beta}_y\delta\beta_x+\beta_x\frac{\partial\delta\beta_y}{\partial t}\right)\right]dx \tag{12}$$

where, the gyroscopic effect is denoted by $2\Omega I_P \beta_x \dot{\beta}_y$ and rotary inertia effect is represented by $I_d\left(\dot{\beta}_x^{\,2}+\dot{\beta}_y^{\,2}\right)$. As the term $\Omega^2 I_d\left(\beta_x^{\,2}+\beta_y^{\,2}\right)$ is very small compared to $\Omega^2 I_p$,it has been neglected in the further analysis. The terms I_m, I_d and I_p are elaborated in the Appendix.

3.4 Kinetic Energy Expression for Disks

In a similar way the kinetic energy expression and the first variation of kinetic energy of the disk are obtained as follows:

$$T_d = \frac{1}{2}\int_0^L \sum_{i=1}^{N_D}\left[I_{mi}^D\left(\dot{v}_0^{\,2}+\dot{w}_0^{\,2}\right)+I_{di}^D\left(\dot{\beta}_x^{\,2}+\dot{\beta}_y^{\,2}\right)-2\Omega I_{pi}^D\beta_x\dot{\beta}_y^{\,2}+\Omega^2 I_{pi}^D\right]\Delta\left(x-x_{Di}\right)dx \tag{13}$$

$$\delta T_d = \int_0^L \sum_{i=1}^{N_D}\left[I_{mi}^D\left(\dot{v}_0\frac{\partial\delta v_0}{\partial t}+\dot{w}_0\frac{\partial\delta w_0}{\partial t}\right)+I_{di}^D\left(\dot{\beta}_x\frac{\partial\delta\beta_x}{\partial t}+\dot{\beta}_y\frac{\partial\delta\beta_y}{\partial t}\right)-\Omega I_{pi}^D\left(\dot{\beta}_y\delta\beta_x+\beta_x\frac{\partial\delta\beta_y}{\partial t}\right)\right]\Delta\left(x-x_{Di}\right)dx \tag{14}$$

Where, disks position denotes by *i* (=1, 2, 3….) and the symbol $\Delta\left(x-x_{Di}\right)$ denotes the one dimensional spatial Dirac delta function.

3.5 Work Done Expression Due to External Loads and Bearings

Here R_y and R_z are assumed as the external force intensities (force per unit length) subjected to the shaft and M_x, M_y are the externally applied torque intensities (moment per unit length) distributed along the shaft. Now virtual work done by the external loads can be represented as follows:

$$\delta W_E = \int_0^L\left(R_y\delta v_0+R_z\delta w_0+M_y\delta\beta_y+M_x\delta\beta_x\right)dx \tag{15}$$

In the present analysis, bearings are modeled by springs and viscous dampers. Virtual work done by springs and dampers can be obtained as,

$$\delta W_B = \int_0^L \sum_{i=1}^{N_B} \begin{pmatrix} -K_{yy}^{Bi} v_0 \delta v_0 - K_{zy}^{Bi} v_0 \delta w_0 - K_{yz}^{Bi} w_0 \delta v_0 - K_{zz}^{Bi} w_0 \delta w_0 \\ -C_{yy}^{Bi} \dot{v}_0 \delta v_0 - C_{zy}^{Bi} \dot{v}_0 \delta w_0 - C_{yz}^{Bi} \dot{w}_0 \delta v_0 - C_{zz}^{Bi} \dot{w}_0 \delta w_0 \end{pmatrix} \Delta(x - x_{Bi}) dx \tag{16}$$

The governing equations of the spinning shaft system can be obtained using equations. (9), (11), (13), (14), (15) and applying Hamilton's principle which is,

$$\int_{t1}^{t2} \left[\delta(T_s + T_d) - \delta U_s + \delta W_E + \delta W_B \right] dt = 0 \tag{17}$$

After simplifying and arranging the above equation, the equations of motions can be obtained as,

$$\delta v_0 : \mathrm{I_m} \frac{\partial^2 v_0}{\partial t^2} + k_s \left(A_{55} + A_{66} \right) \left(\frac{\partial \beta_y}{\partial x} - \frac{\partial^2 v_0}{\partial x^2} \right) + \frac{1}{2} k_s A_{16} \frac{\partial^2 \beta_x}{\partial x^2} + \sum_{i=1}^{N_D} \mathrm{I}_{mi}^D \frac{\partial^2 v_0}{\partial t^2} \Delta\left(x - x_{Di} \right) + P_{v_0}^b = R_y$$

$$\delta w_0 : \mathrm{I_m} \frac{\partial^2 w_0}{\partial t^2} - k_s \left(A_{55} + A_{66} \right) \left(\frac{\partial^2 w_0}{\partial x^2} + \frac{\partial \beta_x}{\partial x} \right) + \frac{1}{2} k_s A_{16} \frac{\partial^2 \beta_y}{\partial x^2} + \sum_{i=1}^{N_D} \mathrm{I}_{mi}^D \frac{\partial^2 w_0}{\partial t^2} \Delta\left(x - x_{Di} \right) + P_{w_0}^b = R_z$$

$$\delta \beta_y : I_d \frac{\partial^2 \beta_y}{\partial t^2} - I_p \Omega \frac{\partial \beta_x}{\partial t} + \frac{1}{2} k_s A_{16} \frac{\partial^2 w_0}{\partial x^2} - B_{11} \frac{\partial^2 \beta_y}{\partial x^2} - k_s \left(A_{55} + A_{66} \right) \left(\beta_x - \frac{\partial v_0}{\partial x} \right) + \sum_{i=1}^{N_D} \left(I_{di}^D \frac{\partial^2 \beta_y}{\partial t^2} - \Omega \mathrm{I}_{pi}^D \frac{\partial \beta_x}{\partial t} \right) \Delta\left(x - x_{Di} \right) = M_y$$

$$\delta \beta_x : I_d \frac{\partial^2 \beta_x}{\partial t^2} - I_p \Omega \frac{\partial \beta_y}{\partial t} + \frac{1}{2} k_s A_{16} \frac{\partial^2 v_0}{\partial x^2} - B_{11} \frac{\partial^2 \beta_x}{\partial x^2} - k_s \left(A_{55} + A_{66} \right) \left(\frac{\partial w_0}{\partial x} + \beta_x \right) + \sum_{i=1}^{N_D} \left(I_{di}^D \frac{\partial^2 \beta_x}{\partial t^2} - \Omega \mathrm{I}_{pi}^D \frac{\partial \beta_y}{\partial t} \right) \Delta\left(x - x_{Di} \right) = M_x$$

3.6 FE Modeling of FRP Composite Shaft

Here, finite element analysis is aiming to find out the field variable (displacement) at nodal points by approximate analysis. In the present FE model, the three-nodded one-dimensional line elements are consider, each node having four degree of freedom (DOF). The Lagrangian interpolation functions are used to approximate the displacement fields of shaft. The element's nodal DOF at each node is v_0, w_0, β_x and β_y. Now displacement field variable can be represented as,

$$v_0 = \sum_{k=1}^{n} v_0^k(t) \psi_k(\eta),\ w_0 = \sum_{k=1}^{n} w_0^k(t) \psi_k(\eta),\ \beta_x = \sum_{k=1}^{n} \beta_x^k(t) \psi_k(\eta),\ \beta_y = \sum_{k=1}^{n} \beta_y^k(t) \psi_k(\eta) \tag{18}$$

Now one dimensional Lagrange polynomial is defined as,

$$L_k(\eta) = \prod_{\substack{m=1 \\ m \neq k}}^{n} \frac{\eta - \eta_m}{\eta_k - \eta_m} \tag{19}$$

For three nodded element, the shape functions or interpolating functions can be expressed as,

$$\psi_1 = \frac{-\eta(1-\eta)}{2},\ \psi_2 = 1-\eta^2,\ \psi_3 = \frac{\eta(1+\eta)}{2}$$

Now putting the displacement field variables and shape function expressions into governing equations, the equation of motion for a element can be written as,

$$[M]\{\ddot{q}\} + ([C] + \Omega[G])\{\dot{q}\} + [K]\{q\} = \{F\} \tag{20}$$

The rotor dynamics equation of motion including both internal viscous and hysteretic can be extended as

$$[M]\{\ddot{q}\} + ([C] + \Omega[G] + \eta_V[K])\{\dot{q}\} + \left[\left(\frac{1+\eta_H}{\sqrt{1+\eta_H^2}}\right)[K] + \left(\eta_V\Omega + \frac{\eta_H}{\sqrt{1+\eta_H^2}}\right)[K_{Cir}]\right]\{q\} = \{F\} \tag{21}$$

The equation of motion of the FRP composite shaft can be obtained after assembly of all the elemental matrices.

where, $[M],[C],[G],[K],\{q\}$ all elemental matrices are given in Appendix.

CHAPTER-4

MATHEMATICAL MODELLING OF ACTIVE MAGNETIC BEARING

A magnetic bearing is used to carry a load by magnetic levitation technique. The main advantage of the bearing is that it runs without any surface contact with the stator, hence the operation is friction less. Magnetic bearings can run at higher speeds without any problem of mechanical wear.

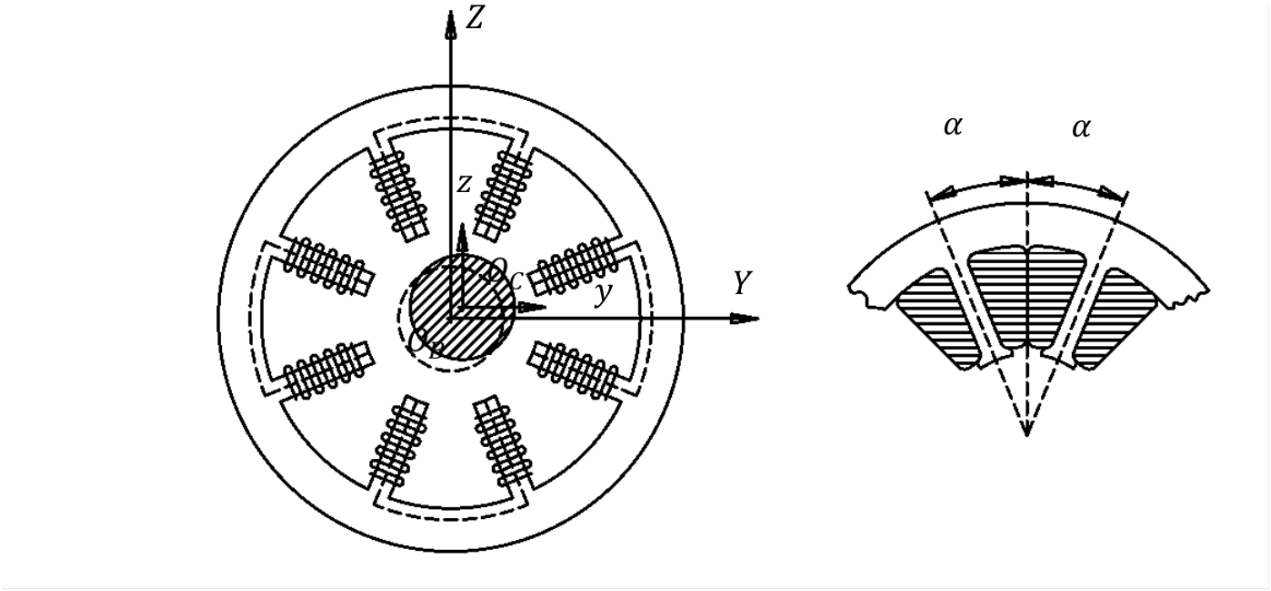

(a) (b)

Fig. 1. Geometrical representation of the stator, electromagnets and the included angle for AMB

The principle of working of the magnetic bearing is to provide suspension through electromagnetic current. For this purpose a complete electromagnet assembly is used. Two power amplifiers, one controller and two gap sensors are used in the assembly. The power amplifier sends control current to the electromagnet while the set of gap sensors and controller

provides the control feedback according to position of the moving rotor within the gap Equal bias currents are sent from the power amplifier into the electromagnet from two opposite directions of the rotor. Function of controller is to add the bias current with positive and negative values of control currents as the rotor changes its center position while running as shown in the Fig 1.

4.1 The Electromagnetic Force

The detail description of the magnetic force created inside the electromagnet is given in detail below.

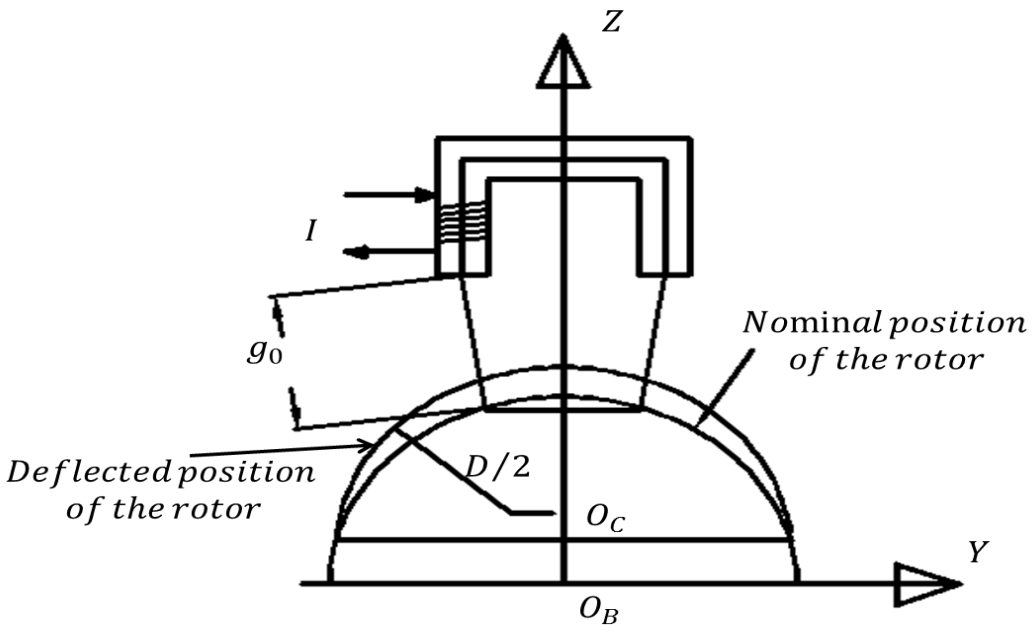

Fig. 2. Diagram showing magnetic circuit formed between shaft and electromagnet

The above Fig. 2 is clearly showing how a magnetic circuit comes into existence in between the rotor and electromagnet when current is passed through the electromagnet. O_B and O_C are the centers of the shaft at its nominal (shaft is stationary) and the deflected positions. Some assumptions are taken into consideration like (1) the gap between rotor and stator is very

small as compared to the radius of the rotor (2) Fringing effect as well as flux leakage is negligible at the pole face.(3) the length of lines of magnetic flux are equal (4) Flux density and the intensity of the the magnetic field of the material follow a linear relationship (5) Magnetic permeability is constant within the operating range (6) lastly, magnetic hysteresis of the material is also assume to be negligible.

$$F_{mag} = - \frac{\varepsilon \mu_0 A_g N^2 i_0^2}{4 g_0^2} \quad (22)$$

where μ_o, A_g, N , i_o and g_o are the absolute permeability of free air, face area of pole, and number of turns of coil, current and initial gap between the rotor and stator respectively. The force increases as the gap decreases due to negative sign in the equation.

As the rotor starts rotating with its centre O_B, it has uniform air gap g_o and bias current of magnitude i_0 flows steadily through the coils of the electromagnet initially but as the time passes the eccentricity developed and the center of the rotor changes. Unbalance magnetic forces start developing inside the rotor-shaft system due to the change in the position of the rotor, when it comes closer to one pair of pole, it goes farther from the opposite one. Because magnetic force is inversely proportional to the square of the gap exist between the rotor and shaft, the control force is necessary to keep the constant gap. The control force inside the system develops according to the gap between rotating and stationary parts. Deflection of the rotor either in Y or Z direction can be controlled by supplying appropriate control current. If the shaft comes closer to one pole of electromagnet, the current is reduced in order to decrease the magnetic force value. Simultaneously the shaft goes farther from the opposite pole of the same electromagnet, the magnetic force is increased by increasing the control current. The forces in either Y or Z directions are completely uncoupled.

4.2 Force, Position Stiffness and Damping Stiffness of Magnetic Bearing

A single axis (along y direction) within the active magnetic bearing actually consists of one pair of horseshoe type magnet as shown in the Fig.3.

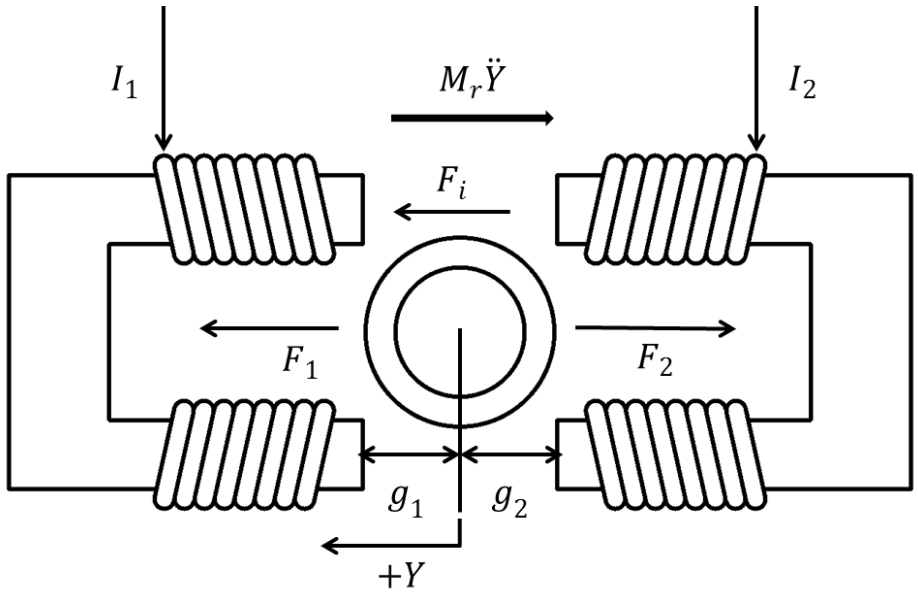

Fig.3 Single axis lay out of active magnetic bearing

F_1 and F_2 are the forces acting within the single axis. The equation of motion of the system can be written as:

$$M_r\ddot{y} + F_2 - F_1 = F_i \tag{23}$$

Now the net force is given by

$$F_{net} = F_2 - F_1 \tag{24}$$

Substituting the value of equation (1) into equation (3) gives

$$F_{net} = \frac{\varepsilon\mu_0 A_g N^2}{4}\left(\frac{I_2^2}{g_2^2} - \frac{I_1^2}{g_1^2}\right) \tag{25}$$

Where the currents in magnet 1 and 2 can be represented as

$$I_1 = i_0 - i_{cY} \tag{26}$$

$$I_2 = i_0 + i_{cY} \tag{27}$$

The gap terms can be replaced by the following

$$g_1 = g_0 - y \tag{28}$$

$$g_2 = g_0 + y \tag{29}$$

Thus the equation becomes

$$F_{net} = \frac{\varepsilon \mu_0 A_g N^2}{4}\left(\left(\frac{i_0 - i_{cY}}{g_0 - y}\right)^2 - \left(\frac{i_0 + i_{cY}}{g_0 + y}\right)^2\right) \tag{30}$$

The equation (30) is a nonlinear equation. To linearize it, the control current i_{cY} and the control position y are considered to be very small as compared to a bigger value of bias current i_0.It makes the equation (30) a linear and a simplified one by not taking the higher order terms of control current i_{cY} (=I_P) and control position y. the equation can be written as

$$F_{net} = \frac{\varepsilon \mu_0 A_g N^2 i_0}{g_0^2} I_p - \frac{\varepsilon \mu_0 A_g N^2 i_0^2}{g_0^3} y \tag{31}$$

The above equation (31) is used to find the position stiffness and current stiffness for the horse shoe type magnet. The position stiffness is obtained by taking partial derivative of the force value F_{net} with respect to control position y at the particular value of gap g_0 and bias current i_0. The current stiffness is also obtained in the same way by taking partial derivative of F_{net} with respect to the control position y. The position stiffness for the horse shoe type magnet can be clearly shown as

$$k_P = \left.\frac{\partial F_{net}}{\partial y}\right|_{g_{0,}\, I_B} = -\frac{\varepsilon \mu_0 A_g N^2 i_0^2}{g_0^3} \tag{32}$$

The corresponding current stiffness can be written as

$$k_I = \left.\frac{\partial F_{net}}{\partial i_{cY}}\right|_{g_{0,}\, I_B} = \frac{\varepsilon \mu_0 A_g N^2 i_0}{g_0^2} \tag{33}$$

Now taking into consideration the included angle '2α' between the poles of electromagnets of active magnetic bearing as shown in the figure(1), the equation becomes

$$K_{P,Y} = -\frac{\varepsilon \mu_0 A_g N^2 i_0^2}{g_0^3}\cos(\alpha) \tag{34}$$

And

$$K_{I,Y} = \frac{\varepsilon \mu_0 A_g N^2 i_0}{g_0^2}\cos(\alpha) \tag{35}$$

Substituting the above values in the equation (23), we get

$$\boldsymbol{M}_r \ddot{\boldsymbol{y}} + \boldsymbol{K}_{PY}\boldsymbol{y} + \boldsymbol{K}_{IY}\boldsymbol{I}_P = \boldsymbol{F}_i \tag{36}$$

Putting the values of K_{PY} and K_{IY} from equation (34, 35) in equation (36),

$$M_r \ddot{y} - \frac{\varepsilon \mu_0 A_g N^2 i_0^2}{g_0^3}\cos(\alpha)\dot{y} + \frac{\varepsilon \mu_0 A_g N^2 i_0}{g_0^2}\cos(\alpha) I_P = F_i \tag{37}$$

The geometry of the figure clearly exhibits that the forces in the Y and Z directions are completely uncoupled and can be calculated separately. Therefore, considering the Z direction the equation can be obtained in the above similar way and can be written as:

$$M_r \ddot{z} - \frac{\varepsilon \mu_0 A_g N^2 i_0^2}{g_0^3}\cos(\alpha)\dot{z} + \frac{\varepsilon \mu_0 A_g N^2 i_0}{g_0^2}\cos(\alpha) I_P = F_i \tag{38}$$

Hence,

$$K_P = K_{P,Y} = K_{P,Z} = -\frac{\varepsilon \mu_0 A_g N^2 i_0^2}{g_0^3} \cos(\alpha) \tag{39}$$

And

$$K_I = K_{I,Y} = K_{I,Z} = \frac{\varepsilon \mu_0 A_g N^2 i_0}{g_0^2} \cos(\alpha) \tag{40}$$

As the position stiffness is negative, it shows that the electro-magnetic force is attractive in nature and it is also inversely proportional to the square of the gap between the rotor and electromagnet. Hence this force keeps on increasing with time and makes the composite rotor shaft system unstable. Therefore, active control system is applied to bring stability to the system.

4.3 Controller Transfer Function, Stiffness and Damping

The controller added in the magnetic bearing makes the whole system to act in an active way. The positive current stiffness discussed earlier provides stability to the active magnetic bearing system. The function of controller is to make variation in the control current to feed to the electromagnets when there is a detection of change in the position of shaft. This change is detected with the help of a sensor fitted in the stator part. Hence, the complete transfer function is actually a ratio of control current to the input of changed position of the shaft. The controller transfer function is a complex valued function as it shows phase information with respect to the signal of input position. Therefore it can be written as:

$$G(i\omega) = a_G(\omega) + i(b_G) \tag{41}$$

where a_G and b_G shows the real part and imaginary part of the complete transfer function respectively, and forcing frequency is denoted by ω. The control current I_{cY} is obtained by multiplying the transfer function with the position y. Now the main equation can be written as:

$$-M_r y\omega^2 + (K_P + K_I(a_G + ib_G))y = F_i \tag{42}$$

The above equation considers a harmonic force function and the mass acceleration is shown by - $y\omega^2$ The net force produced by position stiffness, control current stiffness and by transfer function is said to be equal to the force arise by an equivalent set of stiffness and damping. Now if we equate the two forces it will be shown as

$$(K_P + K_I(a_G + ib_G))y = (K_{eq} + C_{eq} i\omega)y \tag{43}$$

Now if we equate different terms of the equation carefully, we get the equivalent stiffness about one axis as;

$$K_{eq} = K_P + K_I a_G \tag{44}$$

And equivalent axis damping is

$$C_{eq} = \frac{K_I b_G}{\omega} \tag{45}$$

The above equations represent the stiffness and damping values for active magnetic bearing which changes with the speed of the rotor. This is because of their dependency on real part as well as imaginary part of the complete controller transfer function. Therefore a complete transfer function is required to get the values of stiffness and damping.

4.4 Mathematical Modeling of Controller

4.4.1 Introduction

A controller is used here for the active control of the FRP rotor shaft system. In the controller there are several actions take place that should be taken under consideration for proper modeling of the system and to get an appropriate transfer function. One bearing consists of four pairs of electromagnetic pole which are placed around the periphery of the rotor in a symmetric way. Only two control axes along Y and Z direction are considered for the calculation purpose. Figure (3) is showing a block diagram for a radial active magnetic bearing with the controller and other electronic devices like sensor and amplifier. There are different types of operations take place within the controller to achieve a proper control of magnetic bearing stability.

The reference signal is set to zero in the AMB system to align the rotor within the axes of the rotor. Hence this particular input feed can be ignored in the controller function. The controller used here is a digital electronic device. Therefore the position signal coming out from the differential sensor in the voltage form is required to be changed into digital form before sending it to the system controller. An analog to digital converter is used for this purpose. The process of digitization does not affect the overall control of the system, therefore it is ignored. The whole process is well described in Fig. 4.

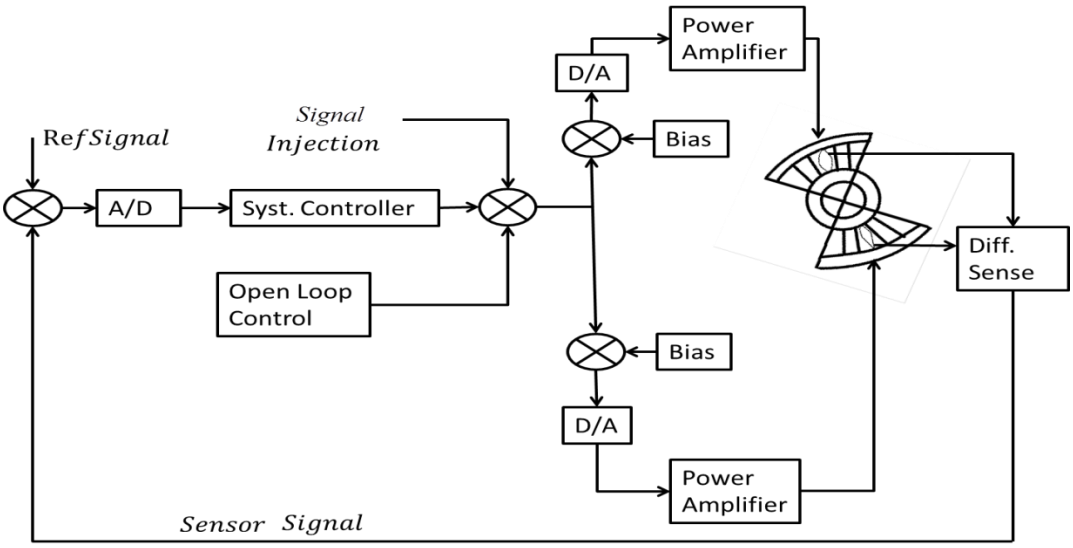

Fig. 4. Block diagram showing the closed loop control for single axis AMB.

The block diagram in Fig. 5 is a simplified one, neglecting the open loop control, signal injection, analog-digital converter and digital-analog converter which are discussed above. The signal taken as a reference is first set to a zero value. Therefore this system input is ignored and the position input is taken in consideration as well. The stiffness and damping coefficient can be determined from the feed through transfer function, G(s), which is discussed above in the section. Hence a simplified block diagram to find out axis stiffness and damping coefficient values is shown in the fig.6.

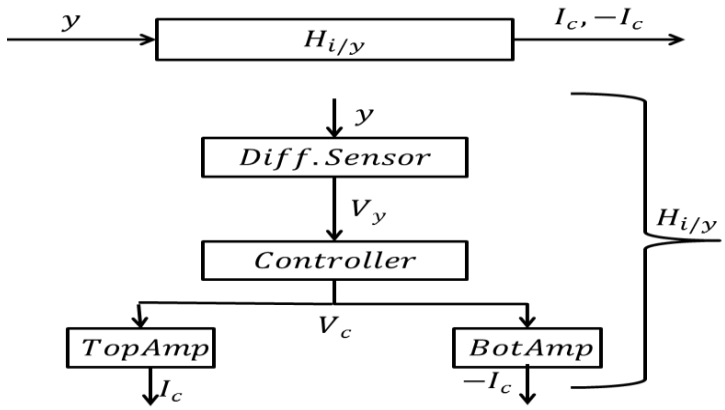

Fig. 5. Simplified block diagram of single control axis

Both amplifiers one at the top and one at the bottom receive the same amount of signal as control voltage and convert it into same control current, I_C , which differs in sign only. The top electromagnet receives a reduction in current when the rotor position detects positive displacement toward the top magnets in the stator and the bottom magnet receive an increase in current to pull the rotor back into the centered position.

In the present study a combination of filters like PID, notch and low pass are used to control the FRP composite shaft assembly and that becomes the basis behind control strategy of the system controller. Figure 6 gives a block diagram where the system controller is replaced by these three filters. One power amplifier is shown due to its equivalence property discussed earlier.

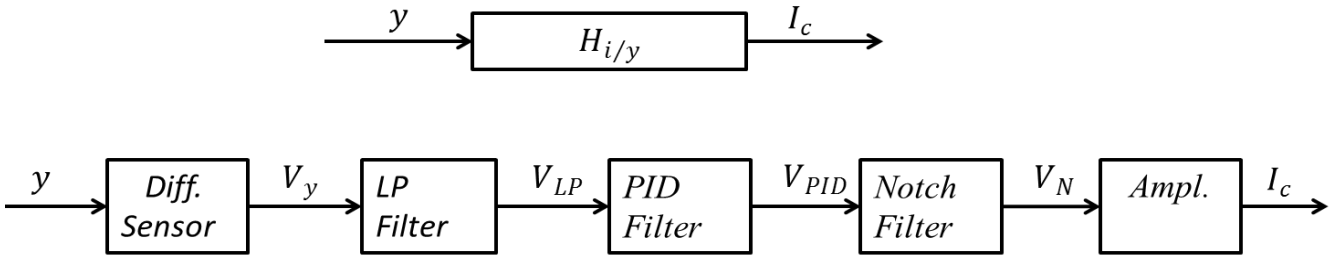

Fig. 6. Open loop control block diagram for one pole of electromagnets

The above block diagram is showing a complete transfer function G(s) which has been discussed earlier and it is consisting of different elements like differential sensor, low pass filter, PID filter, notch filter and amplifier. The individual component of the transfer function is modeled in detail in the following section.

$$G(s) = S(s)LP(s)PID(s)N(s)AMP(s) \tag{46}$$

where s is defined as the complex frequency variable. It can be changed with '$i\omega$'.

4.4.2 Differential Sensor

The main function of differential sensor is to sense the deflection of the rotor within the axis from the set point of controller. For the simplicity point of view the set point is set to zero. Therefore the differential sensor simply measures the position change of the rotor from the center of the axis. The differential sensor is modeled to give a gain value relating to output voltage of sensor and the measured position of differential. This gain or sensor sensitivity is user defined and set to 0.1572 Volts/mil. This value is determined by measuring the inside diameter of the stator and recording the corresponding output voltage of the stator when the rotor was against one magnet. Now the sensitivity is determined as the ratio of output voltage to the radial clearance. Also the sensor is assume to behave linearly at all the frequency ranges within the rotor .The sensor transfer function can be written as

$$SS(s) = \frac{V_y}{y} = 0.1572 \tag{47}$$

4.4.3 Low Pass Filter

The low pass filter must be used within the system controller for the bearing to operate properly as it is used to attenuate the electrical noise due to high frequency and also reduce the controller's high frequency gain above the bandwidth of the hardware. However by doing so, resonance at high frequency may not be controlled properly. To model the low pass filter, a second order low pass filter is used where V_{LP} is the output voltage of the filter. V_y is the input position signal in volts while ω_{LP} and ξ_{LP} is the cutoff frequency and filter damping ratio respectively. s is the complex frequency variable. A second order low pass filter of the form

$$LP(s) = \frac{V_{LP}}{V_y} = \frac{\omega_{LP}^2}{s^2 + 2\xi_{LP}\omega_{LP}s + \omega_{LP}^2} \quad (48)$$

4.4.4 Proportional, Integral, and Derivative Filter

The combination of proportional control action, integral control action, and derivative control action is termed proportional-plus-integral-plus-derivative control action and is accordingly sometimes called three-term control. It has the advantages of each of the three individual control actions. A PID controller calculates an "error" value as the difference between a measured process variable and a desired set point. The controller attempts to minimize the error in outputs by adjusting the process control inputs. *P* depends on the *present* error, *I* on the accumulation of *past* errors, and *D* is a prediction of *future* errors, based on current rate of change. By tuning the three parameters in the PID controller algorithm, the controller can provide control action designed for specific process requirements. Block diagram showing different control actions of a PID filter is shown in the Fig. 7.

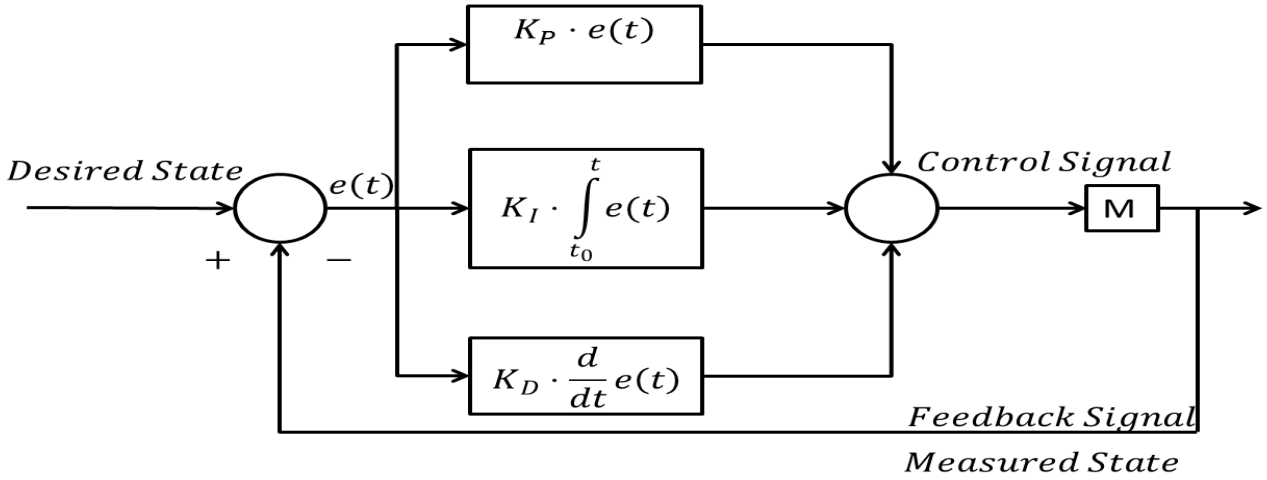

Fig. 7. Block diagram for PID control.

$$u(t) = MV(t) = K_P e(t) + K_I \int_0^t e(\tau) d\tau + K_D \frac{d}{dt} e(t) \tag{49}$$

PID control is the most commonly used control method for magnetic bearings. The standard continuous PID form is given by

$$PID(s) = \frac{V_{PID}}{V_{LP}} = \frac{K_T (K_D s^2 + K_P s + K_I)}{s} \tag{50}$$

where K_P is the Proportional gain, K_I is the Integral gain, K_D *is the* Derivative gain and K_T is the total gain. τ is the variable of integration, e is the error and t is the time. V_{PID} is the output voltage of the filter and V_{LP} is the input voltage from the low pass filter. In general, the proportional gain directly affects the bearing stiffness because it is multiplied by the position signal directly. Similarly, the derivative gain directly affects the damping of the axis because it is multiplied by the derivative of the position signal. The integral gain acts on steady offsets within the axis and provides a control signal to eliminate the offset. The total gain is simply a multiplier on all three gains simultaneously.

4.4.5 Notch Filter

The purpose of notch filter controller is to allow the rotor center of mass is to remain stationary by making the bearings not respond at the rotational frequency. The model used to represent the notch filter can be written as

$$N(s) = \frac{V_N}{V_{PID}} = \frac{s^2 + 2\xi_N \omega_N s + \omega_N^2}{s^2 + 2\omega_N s + \omega_N^2} \tag{51}$$

Where ω_N and ξ_N represent the notch frequency and notch filter damping respectively. s is the complex frequency variable and V_N is the filter output voltage and V_{PID} is the input voltage from the PID filter. Notch filters are used to damp out problematic high frequency resonances above the operating speed or frequency bandwidth of the system.

4.4.6 Power Amplifier

Its main function is to amplify the signal coming from the notch filter and send to the magnets in the form of control current. The power amplifiers used in the controller are switching amplifiers with a switching frequency of 40,000 Hz. Although the effects of these amplifiers in the low frequency range (0-100Hz) are negligible, a model of the frequency response of these amplifiers has been included for completeness and to incorporate the gain associated with the amplifiers. The amplifiers are modeled as a butter-worth second order low pass filter described as below

$$AMP(s) = \frac{I_c}{V_N} = K_a \frac{\omega_a^2}{s^2 + \sqrt{2}\omega_A s + \omega_A^2} \tag{52}$$

where I_c is the control current which is going into the individual magnets, V_N is the input notch filter voltage and s is the complex frequency variable. The switching frequency of 40,000 Hz is taken to be the filter cutoff frequency ω_A and the Amplifier gain, K_a is taken as 900.

4.5 Stability of the System

The role of the system eigenvalues are of utmost importance as it decides whether the system is stable or not. Generally, the eigenvalues are in complex form and its negative real part denotes the stable system, while a non- negative value indicates the instability. Hence the maximum real part of the eigenvalues must be negative for the stable operation of rotor-shaft system at a particular speed.

Therefore, the lowest speed at which the maximum real part changes its sign from a non-negative value to a negative value is termed as stability limit speed (SLS) of the system. The stability limit speed should always be more than the first critical speed of the system. Stability can be achieved by using active magnetic bearing and tuning the optimum combination of different parameters of the PID filter.

CHAPTER-5

RESULTS AND DISCUSSIONS

5.1 Details of FRP composite shaft system

The rotor with AMB, used for the numerical simulation is shown in the figure (). A complete programming is developed using MATLAB 13a to analyze the effectiveness of active control method on the stability of the FRP rotor shaft system. The shaft is loaded with three dishes and is supported with the help of two identical orthotropic bearings. The stiffness and damping coefficients of each bearing are $k_{yy} = 1.75 \times 10^7$ N/m, $k_{zz} = 1.75 \times 10^7$ N/m, $c_{yy} = 500$ N s/m, $c_{zz} = 500$ N s/m.

The FRP rotor shaft is been divided into 13 equal Rayleigh beam finite elements and magnetic bearing is located at the ends of the shaft .The included angle between the poles is taken as $2\alpha = 45^{\circ}$ shown in the Fig. Controller is connected with the bearing and provides active vibration and stability control of the whole system. Bias current for each of the magnets within the magnetic bearing is 0.75 Amps which more closely mimics a power-limited system. A nominal gap of 0.381 mm is maintained initially when no vibration takes place. A low pass filter with a cutoff frequency of 800 Hz and a damping ratio of 0.7 is used along with a PID filter with very low gains to initially levitate the system .A notch filter is also used to dampen out high frequency resonance. It is used at a frequency of 200 Hz which is substantially higher than the first critical speed of the controlled system. Hence it does not affect the stability of the system. The assumed optimum values of control parameters of PID filter are total gain $k_t = .00095$, derivative gain $k_d = .99$, proportional gain $k_d = 0.99$ and integral gain $k_i = 1 \cdot$

Table 1

Parameters of FRP composite shaft system.

Parameter	Shaft	Disk 1	Disk 2	Disk 3
Length	1.2			
Diameter(mm)	100			
Density	1578			
Coefficient of viscous damping	0.0002			
Coefficient of hysteretic damping	0.0002			
Eccentricity (m)		0.0002	0.0002	0.0002
Shear correction factor	0.56			
Mass of disc(kg)		45.947	45.947	45.947
Longitudinal Young's Modulus (GPa)	139			
Transverse Young's Modulus (GPa)	11			
Poisson's Ratio	0.313			

5.2 Comparison Between Controlled and Uncontrolled Responses

The comparisons between the controlled and uncontrolled responses of the FRP composite shaft system are clearly shown in the Fig.8, Fig.9 and Fig.10.These results are obtained by using the stacking sequence [90/45/45/0/0/0/0/0/90].

In the uncontrolled response of the FRP composite shaft system, the bearing stiffness and damping is present along with internal viscous and hysteretic damping of the shafts. On the other hand in the uncontrolled response, additional stiffness and damping values are added to the system in an active way with the use of an active controller discussed earlier.

The Campbell diagram shown in the Fig.8 clearly exhibits that the critical speed of the uncontrolled shaft system is around 3045 rpm, which is increased up to 3814 rpm when active control technique is applied.

Figure 9 shows the variation of damping ratio of the controlled and uncontrolled rotor-bearing system. Six natural modes are being shown where we see that the damping ratio in the uncontrolled case becomes negative around 13600 rpm.

Figure 10 shows the same fact that the stability limit speed can reach up to 13580 rpm with active control system in place.

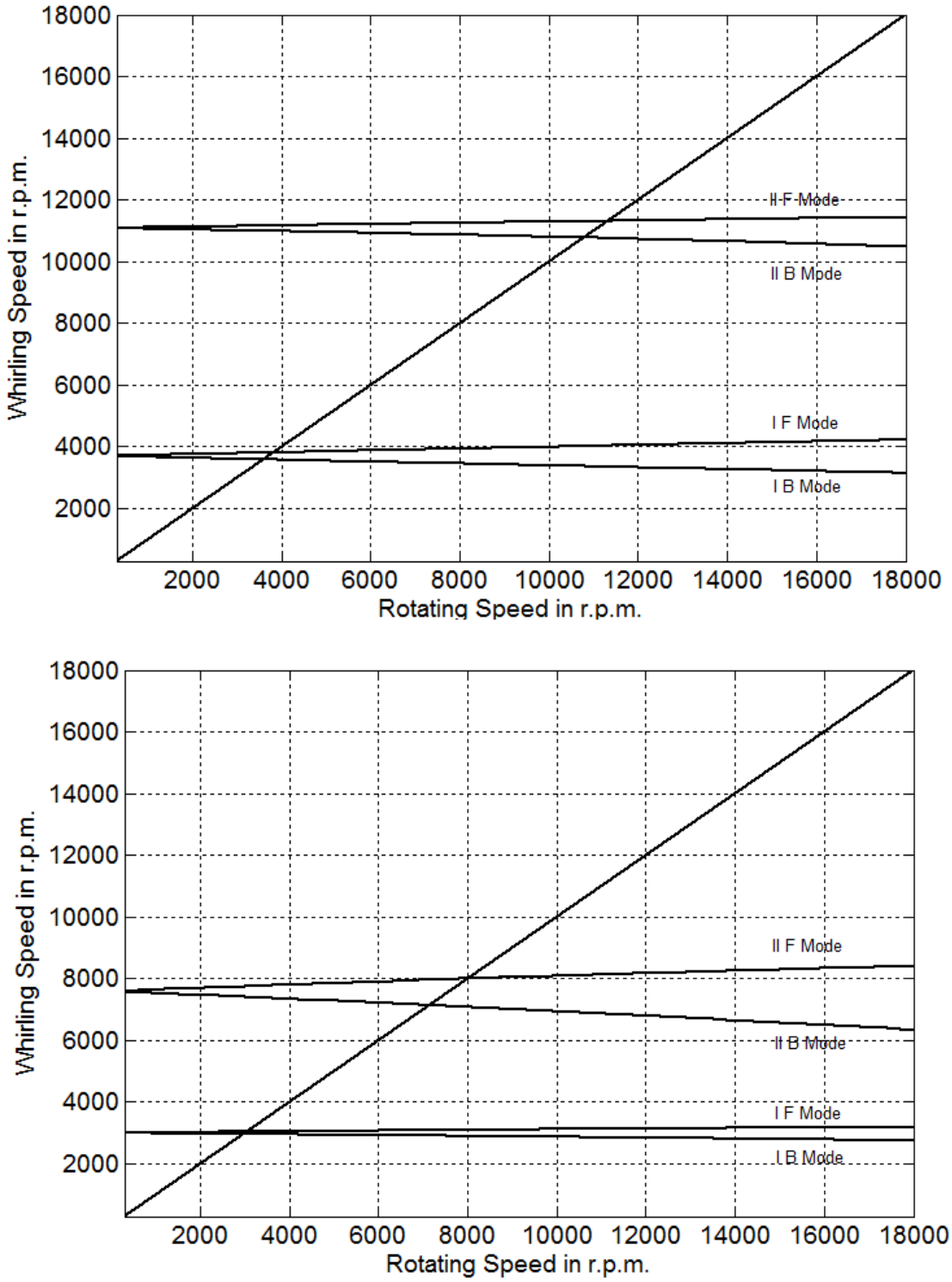

Fig. 8. Comparison of the campbell diagram for uncontrolled (lower fig.) and controlled (upper fig.) system.

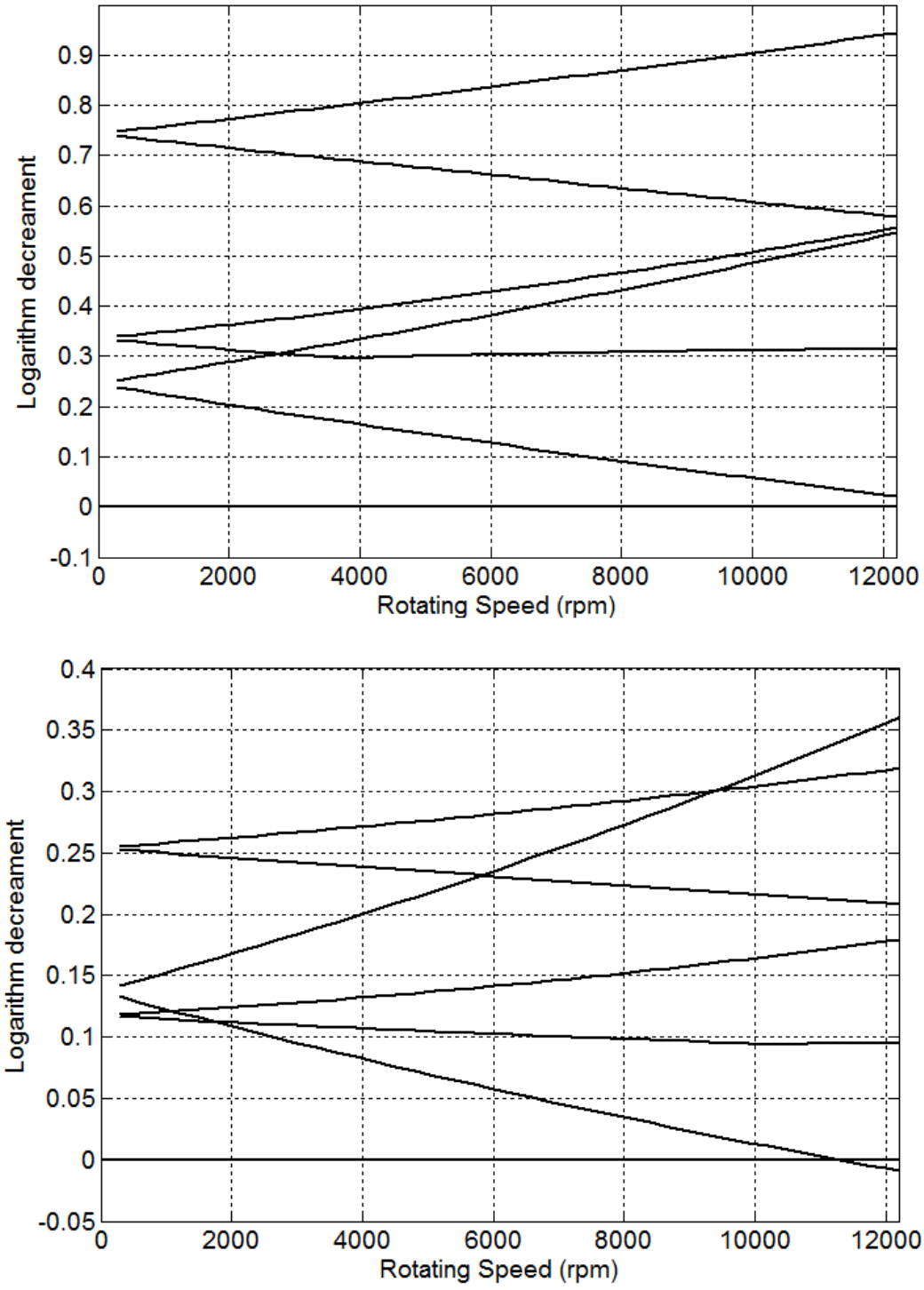

Fig. 9. Variation of damping ratio of first six modes for uncontrolled (lower fig.) and controlled (upper fig.) system.

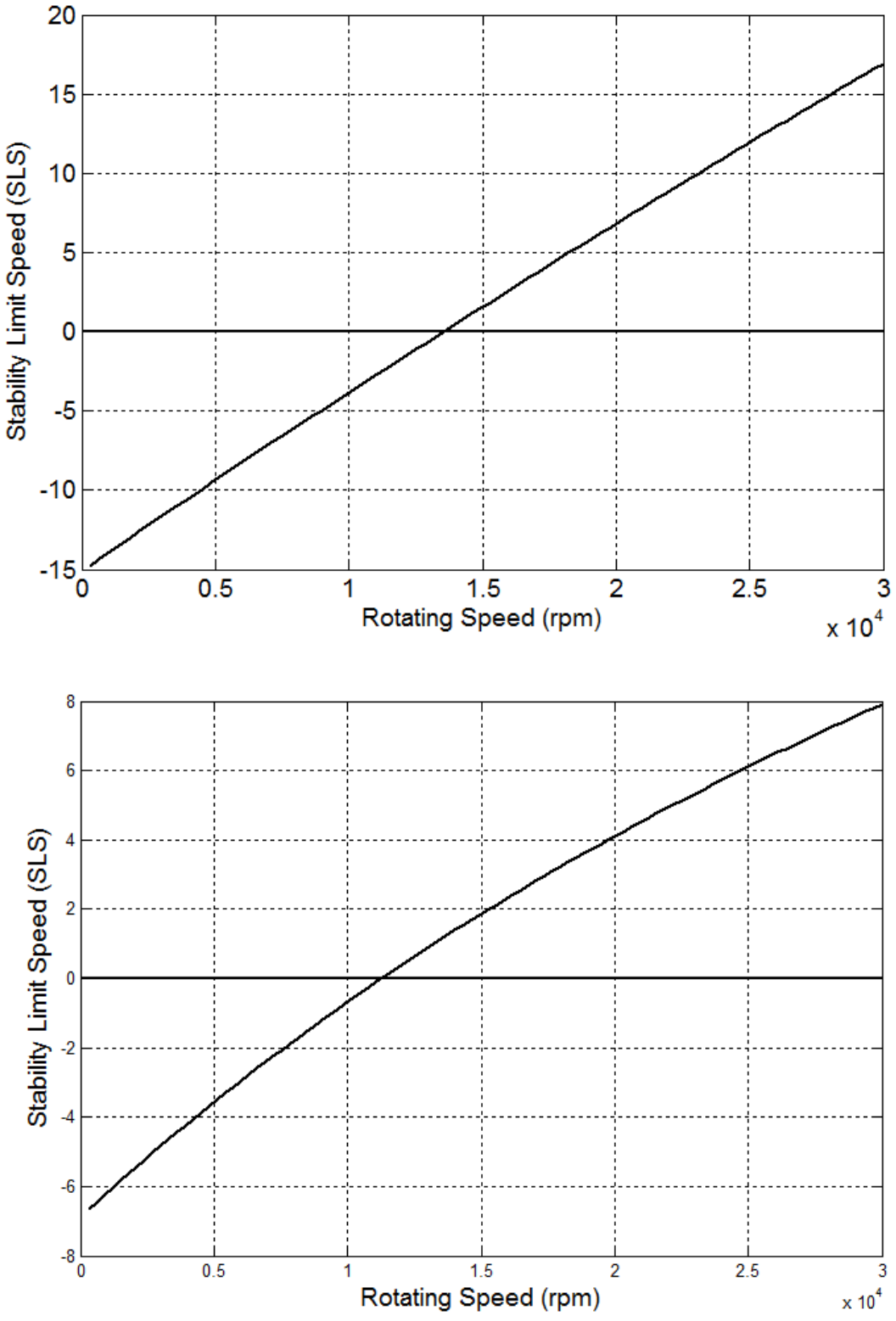

Fig. 10. Variation of maximun real part of the eigenvalues with rotational speed.

5.3 Effect of Stacking Sequences

In Table No.2 different stacking sequences are taken under consideration. In symmetric stacking sequence the stability limit value changes from 2535 rpm to 2627 rpm when active magnetic bearing control is applied. The first critical speed also changes its value from 2405 rpm to 2765 rpm.

In anti-symmetric stacking sequence the critical speed value increases to 3250 rpm from 2731 rpm while stability limit speed increase to 3655 rpm from 3192 rpm.

In the cross sequencing the critical speed changes from 2630 rpm to 3112 rpm. On the other hand stability limit speed increases from 8651 rpm to 9908 rpm.

Table No.2

Comparison of different stacking sequences

Stacking Sequence	Uncontrolled		Controlled	
	Critical Speed (Rpm)	Stability Limit Speed (Rpm)	Critical Speed (Rpm)	Stability Limit Speed (Rpm)
$[90/90/45/0/0]_S$	2405	2535	2765	2627
$[45/0/45/0/90]_{AS}$	2731	3192	3250	3655
[0/90/0/90/0/90/ 0/90/0/90]	2630	8651	3112	9908
[90/45/45/0/ 0/0/0/0/0/ 90]	3045	11260	3814	13580

For the stacking sequence of [90/45/45/0/0/0/0/0/0/90] the controlled response of the FRP composite shaft system is also shown in the table. The critical speed in this case increases from 3045 rpm to 3814 rpm and stability limit speed from 11260 rpm to 13545 rpm. Hence the use of active magnetic bearing controls the stability of the system to a greater extent in this particular stacking sequence.

CHAPTER-6

CONCLUSIONS AND FUTURE WORK

6.1 Conclusion

From the above results it may be concluded that the active magnetic bearing used in the rotor-shaft system where rotor is made up of fiber reinforced polymer (FRP) composite, brings the system into a stable position. The active technique is achieved by bringing a controller into the picture which senses the displacement and controls the corresponding current in order to achieve stability. The different parameters of PID filter are tuned manually to get the optimum results. The Campbell diagrams prove that the critical speed of the controlled system has been increased to a higher value and the stability limit speed (SLS) diagrams show that the system can run at much higher speed when operated with active control method. The active magnetic bearing also provides a contact-free operation which reduces rotor vibration. The control action is free from the problem of maintenance, wear and tear and power loss due to friction.

6.2 Scope of Future Work

- Functionally graded materials (FGM) can be used in place of composite material for the shaft.
- The effect of temperature can also be analyzed to see the variation of the results with respect to different temperature distribution.
- The effect of stresses induced in the lamina of the composite shaft can also be analyzed.

REFERENCES

[1] Singh.S.P., Gupta.K. "Composite Shaft Rotordynamic analysis using a layerwise theory", Journal of Sound and Vibration, vol. 191(5), pp. 739-756, (1996).

[2] Kim.W., Argento.A., and Scott.R.A "Free Vibration of a Rotating Tapered Composite Shaft System", Journal of Sound and Vibration, vol. 226(1), pp. 125-147, (1999).

[3] Chang.M.Y., Chen.J.K., and Chang.C.Y. "A simple Spinning Laminated Composite Shaft Model", International Journal of Solids and Structures, vol. 41, pp. 637-662, (2004).

[4] Ghoneam.S.M., Hamada.A.A., and El-Elamy.M.I. "Dynamic Analysis of Composite Shaft",Department of Production Engineering and Mechanical Design, Menoufia University, Egypt.

[5] Boukhalfa.A., "Dynamic Analysis of a Spinning Laminated CompositeShaft Using the hp-Version of the Finite Element Method", Department of Mechanical Engineering, University of Tlemcen, Algeria.

[6] Richardet.G.J., Chatelet.E., and Baranger.T.N. "Rotating Internal Damping in the Case of Composite Shaft", University de Lyan, CNRS, INSA-Lyan, LaMCoS UMR5259, Velleurbanne F-69621,France.

[7] Chang.M.Y., Chen.J.K., Chang.C.Y., "A simple spinning laminated composite shaft model", Department of Mechanical Engineering, National Chung Hsing University,Taiwan.

[8] Nelson.F.C., "Rotor Dynamics without Equation", Professor of Mechanical Engineering, Tuffts University, Medford, MA 02155, USA.

[9] Perini E.A., Bueno D. D., Santos R. B., Junior V. L., Nascimento Luiz de P. "Rotating Machinery Vibration Control Based on Poles Allocation using Magnetic Actuators"

International Conference on Engineering Optimization, Rio de Janeiro, Brazil, June (2008), pp.1 -5

[10] Bennett, Stuart "A history of control engineering", (1993).

[11] Ang K.H., Chong G.C.Y., and Li Y. "PID control system analysis, design, and technology", IEEE Trans Control Systems Tech, vol.13, no.4, (2005), pp.559-576.

[12] Foeppl A., Der Civilingenieur, "Das Problem der Delaval'schen Turbinenvelle" (1895), pp. 333-342.

[13] Stodola A., "Neve Kristische Drehzahlen als folye der kreisel wirkuag der laufrader" Gesante Tubinenwes, 15, (1918), PP. 269–275.

[14] Jeffcott H. H., "The lateral vibration of loaded shafts in the neighbourhood of the whirling speeds", Philosophical magazine, vol. 37, (1919), pp.304-315.

[15] Kirk R. G., Gunte E. J., "the effect of support flexibility and damping on the synchronous response of a single mass flexible rotor", J. Eng. Ind., Trans. ASME (1972) pp. 221–232.

[16] Nelson, H.D. and McVaugh, J.M., "The Dynamics of Rotor-bearing Systems Using Finite Elements," ASME Journal of Engineering for Industry, Vol. 98,No.2, (1976), pp. 593-600.

[17] Schweitzer G., Bleuler H.A. "Traxler, Active Magnetic Bearings", (1994).

[18] Schweitzer G., "Magnetic bearing for vibration control", in: NASA Conference publication.

[19] Schittenhelm R. S., Borsdorf M., Riemann B., Rinderknecht S. "Linear Quadratic Regulation of a Rotating Shaft being Subject to Gyroscopic Effect" WCECS 2012, October 24-26, San Francisco, USA, (2012).

[20] Lund J.W., "Response characteristics of a rotor with flexible damped supports, dynamics of Rotor", Proceedings of the IUTAM Symposium, Springer-Verlag, Lyngby, Denmark, (1974), pp. 2–16.

[21] Allaire P.E., Humphris R.R., and Kelm R.D., "Rotordynamic instability problems in high-performance turbomachinery", NASA CP-2443, "Dynamics of a flexible rotor in magnetic bearings", (1986), pp. 419-430.

[22] Koroishi E.H., Steffen Jr. V., "Active vibration control using electromagnetic actuator: A simple model approach (Conferencia Brasileira control application)", (2011), pp. 51-54.

[23] Koroishi E. H. , Steffen Jr V. and Mahfoud J. " Fuzzy Control of Rotor System Using an Electromagnetic Actuator" Owned by the authors, published by EDP Sciences, 09003, (2012), pp. 1-6.

[24] Keith F. J. and Allaire P. "Digital control of magnetic bearings supporting a multimass flexible rotor", (1990), Tribology transactions, 33.

[25] Cheung L. Y., Dunn R.W., Daniels A. R. and Berry T. "Active vibration control of rotor systems". (1994), Control 94, IEEE, pp. 1157-1163.

[26] Abduljabbar Z., ELMadany M.M., and AlAbdulwahab A.A. "Computers and Structures", 58 (3), pp.499-511 "Active Vibration Control of a Flexible Rotor", (1996), pp. 75–84.

[27] Roy T., Chakaraborty D. "Optimal vibration control of smart fiber reinforced composite shell structures using improved genetic algorithm" Journal of Sound and Vibration 319 (2009) pp.15–40

[28] Cole M.O.T., Keogh P.S., Burrows C.R., "Control of multi-frequency rotor vibration Components", J. Mech. Eng. Sci., Proc. I. Mech. E C-216 (2002) pp. 165–177.

[29] Jingjun Zhang, Lili He, Ercheng Wang, Ruizhen Gao Hebei "Workshop on Computational Intelligence and Industrial Application", University of Engineering, Handan, Hebei, 05, China, IEEE Pacific-Asia, (2008), pp 60-38,.

[30] Koroishi E. H., Perini E. A., Nascimento L. P., Lopes jr V., Steffen jr V., "Active Vibration Control in Rotor System Using Magnetic Bearing with LQR", Proceedings of the 1st International Congress of Mathematics, Engineering and Society-ICMES 2009.

[31] Janik T.K., Irretier H., "New excitation and response measurement techniques for modal testing of flexible rotors", Proceedings of the IFTOMM Conference on Rotordynamics, Darmstadt, (1998), pp. 695–708.

[32] Dutt J.K., Toi T.,"Rotor vibration reduction with polymeric sectors", J. Sound Vibr., 262 (4), (2003), pp. 769 -793.

[33] Meirovitch L. "Dynamics and Control of Structures", Wiley Interscience, Bracksburg, VA, USA.

[34] Clements J.R., "The Experimental Testing of an Active magnetic Bearing/Rotor System Undergoing Base Excitation", Master"s Thesis, Virginia Polytechnic Institute and State University, Virginia,USA (2000)

APPENDIX

The terms $A_{11}, A_{55}, A_{66}, B_{11}$ of the equation (9) and I_m, I_d, I_p of the equation (11) given as follows:

$$A_{55} = \frac{\pi}{2}\sum_{i=1}^{k}\overline{C}_{55r}\left(r^2{}_{i+1} - r^2{}_{i}\right), \qquad A_{66} = \frac{\pi}{2}\sum_{i=1}^{k}\overline{C}_{66r}\left(r^2{}_{i+1} - r^2{}_{i}\right)$$

$$A_{16} = \frac{2\pi}{3}\sum_{i=1}^{k}\overline{C}_{16r}\left(r^3{}_{i+1} - r^3{}_{i}\right), \qquad B_{11} = \frac{\pi}{4}\sum_{i=1}^{k}\overline{C}_{11r}\left(r^4{}_{i+1} - r^4{}_{i}\right)$$

$$I_m = \pi\sum_{i=1}^{k}\rho_i\left(r^2{}_{i+1} - r^2{}_{i}\right), \quad I_d = \frac{\pi}{4}\sum_{i=1}^{k}\rho_i\left(r^4{}_{i+1} - r^4{}_{i}\right), \quad I_p = \frac{\pi}{2}\sum_{i=1}^{k}\rho_i\left(r^4{}_{i+1} - r^4{}_{i}\right)$$

Elemental nodal displacement vector,

$$\left\{q_e\right\}^T = \left\{\left\{v_e\right\}^T_{1\times3}\left\{w_e\right\}^T_{1\times3}\left\{\beta_{xe}\right\}^T_{1\times3}\left\{\beta_{ye}\right\}^T_{1\times3}\right\}_{1\times12}$$

Elemental mass matrix,

$$\left[M_e\right] = \begin{bmatrix} \left[M_v\right]_{3\times3} & \left[0\right]_{3\times3} & \left[0\right]_{3\times3} & \left[0\right]_{3\times3} \\ \left[0\right]_{3\times3} & \left[M_w\right]_{3\times3} & \left[0\right]_{3\times3} & \left[0\right]_{3\times3} \\ \left[0\right]_{3\times3} & \left[0\right]_{3\times3} & \left[M_{\beta_x}\right]_{3\times3} & \left[0\right]_{3\times3} \\ \left[0\right]_{3\times3} & \left[0\right]_{3\times3} & \left[0\right]_{3\times3} & \left[M_{\beta_y}\right]_{3\times3} \end{bmatrix}_{12\times12}$$

$$\left[M_v\right] = I_m\int_{x_i}^{x_f}\left[\Psi\right]^T\left[\Psi\right]dx + I_m^D\int_{x_i}^{x_f}\sum_{i=1}^{N_D}\left[\Psi\right]^T\left[\Psi\right]\Delta\left(x - x_{Di}\right)dx$$

$$\left[M_w\right] = I_m\int_{x_i}^{x_f}\left[\Psi\right]^T\left[\Psi\right]dx + I_m^D\int_{x_i}^{x_f}\sum_{i=1}^{N_D}\left[\Psi\right]^T\left[\Psi\right]\Delta\left(x - x_{Di}\right)dx$$

$$\left[M_{\beta_x}\right] = I_d\int_{x_i}^{x_f}\left[\Psi\right]^T\left[\Psi\right]dx + I_d^D\int_{x_i}^{x_f}\sum_{i=1}^{N_D}\left[\Psi\right]^T\left[\Psi\right]\Delta\left(x - x_{Di}\right)dx$$

$$\left[M_{\beta_y}\right] = I_d \int_{x_i}^{x_f} \left[\Psi\right]^T \left[\Psi\right] dx + I_d^D \int_{x_i}^{x_f} \sum_{i=1}^{N_D} \left[\Psi\right]^T \left[\Psi\right] \Delta\left(x - x_{Di}\right) dx$$

Elemental stiffness matrix

$$\left[K_e\right] = \begin{bmatrix} \left[K_{vv}\right]_{3\times3} & \left[0\right]_{3\times3} & \left[K_{v\beta_x}\right]_{3\times3} & \left[K_{v\beta_y}\right]_{3\times3} \\ \left[0\right]_{3\times3} & \left[K_{ww}\right]_{3\times3} & \left[K_{w\beta_x}\right]_{3\times3} & \left[K_{w\beta_y}\right]_{3\times3} \\ \left[K_{v\beta_x}\right]_{3\times3}^T & \left[K_{w\beta_x}\right]_{3\times3}^T & \left[K_{\beta_x\beta_x}\right]_{3\times3} & \left[K_{\beta_x\beta_y}\right]_{3\times3} \\ \left[K_{v\beta_y}\right]_{3\times3}^T & \left[K_{w\beta_y}\right]_{3\times3}^T & \left[K_{\beta_x\beta_y}\right]_{3\times3}^T & \left[K_{\beta_y\beta_y}\right]_{3\times3} \end{bmatrix}_{12\times12}$$

$$\left[K_{vv}\right] = \int_{x_i}^{x_f} \left\{ K_s \left(A_{55} + A_{66}\right) \left[\Psi'\right]^T \left[\Psi'\right] + \sum_{i=1}^{N_B} K_{yy}^{Bi} \left[\Psi\right]^T \left[\Psi\right] \Delta\left(x - x_{Bi}\right) \right\} dx$$

$$\left[K_{ww}\right] = \int_{x_i}^{x_f} \left\{ K_s \left(A_{55} + A_{66}\right) \left[\Psi'\right]^T \left[\Psi'\right] + \sum_{i=1}^{N_B} K_{zz}^{Bi} \left[\Psi\right]^T \left[\Psi\right] \Delta\left(x - x_{Bi}\right) \right\} dx$$

$$\left[K_{\beta_x\beta_x}\right] = \int_{x_i}^{x_f} \left\{ K_s \left(A_{55} + A_{66}\right) \left[\Psi\right]^T \left[\Psi\right] + D_{11} \left[\Psi'\right]^T \left[\Psi'\right] \right\} dx$$

$$\left[K_{\beta_y\beta_y}\right] = \int_{x_i}^{x_f} \left\{ K_s \left(A_{55} + A_{66}\right) \left[\Psi\right]^T \left[\Psi\right] + D_{11} \left[\Psi'\right]^T \left[\Psi'\right] \right\} dx$$

$$\left[K_{v\beta_x}\right] = \left(-\frac{1}{2} K_s B_{16} \right) \int_{x_i}^{x_f} \left[\Psi'\right]^T \left[\Psi'\right] dx$$

$$\left[K_{v\beta_y}\right] = -K_s \left(A_{55} + A_{66}\right) \int_{x_i}^{x_f} \left[\Psi'\right]^T \left[\Psi\right] dx$$

$$\left[K_{w\beta_x}\right] = K_s \left(A_{55} + A_{66}\right) \int_{x_i}^{x_f} \left[\Psi'\right]^T \left[\Psi\right] dx$$

$$\left[K_{w\beta_y}\right]=\left(-\frac{1}{2}K_s B_{16}\right)\int_{x_i}^{x_f}\left[\Psi'\right]^T\left[\Psi'\right]dx$$

$$\left[K_{\beta_x\beta_y}\right]=\frac{1}{2}K_s B_{16}\int_{x_i}^{x_f}\left\{\left[\Psi'\right]^T\left[\Psi\right]-\left[\Psi\right]^T\left[\Psi'\right]\right\}dx$$

Elemental damping matrix of bearing

$$\left[C_e^B\right]=\begin{bmatrix}\left[C_v\right]_{3\times3} & \left[0\right]_{3\times3} & \left[0\right]_{3\times3} & \left[0\right]_{3\times3}\\ \left[0\right]_{3\times3} & \left[C_w\right]_{3\times3} & \left[0\right]_{3\times3} & \left[0\right]_{3\times3}\\ \left[0\right]_{3\times3} & \left[0\right]_{3\times3} & \left[0\right]_{3\times3} & \left[0\right]_{3\times3}\\ \left[0\right]_{3\times3} & \left[0\right]_{3\times3} & \left[0\right]_{3\times3} & \left[0\right]_{3\times3}\end{bmatrix}_{12\times12}$$

$$\left[C_v\right]=\int_{x_i}^{x_f}\sum_{i=1}^{N_B}C_{yy}^{Bi}\left[\Psi\right]^T\left[\Psi\right]\Delta\left(x-x_{Bi}\right)dx,\quad\left[C_w\right]=\int_{x_i}^{x_f}\sum_{i=1}^{N_B}C_{zz}^{Bi}\left[\Psi\right]^T\left[\Psi\right]\Delta\left(x-x_{Bi}\right)dx$$

Elemental gyroscopic matrix,

$$\left[G_e\right]=\begin{bmatrix}\left[0\right]_{3\times3} & \left[0\right]_{3\times3} & \left[0\right]_{3\times3} & \left[0\right]_{3\times3}\\ \left[0\right]_{3\times3} & \left[0\right]_{3\times3} & \left[0\right]_{3\times3} & \left[0\right]_{3\times3}\\ \left[0\right]_{3\times3} & \left[0\right]_{3\times3} & \left[0\right]_{3\times3} & \left[G_{\beta_x\beta_y}\right]_{3\times3}\\ \left[0\right]_{3\times3} & \left[0\right]_{3\times3} & \left[-G_{\beta_x\beta_y}\right]_{3\times3}^T & \left[0\right]_{3\times3}\end{bmatrix}_{12\times12}$$

$$\left[G_{\beta_x\beta_y}\right]=I_P\int_{x_i}^{x_f}\left[\Psi\right]^T\left[\Psi\right]dx+I_P^D\int_{x_i}^{x_f}\sum_{i=1}^{N_D}\left[\Psi\right]^T\left[\Psi\right]\Delta\left(x-x_{Di}\right)dx$$

Elemental circulation matrix $\left[K_{Cir}\right]_{12\times12}=\int_{x_i}^{x_f}M^T\xi M dx$

Where,

$$M = \begin{bmatrix} \psi_1^{'} & \psi_2^{'} & \psi_3^{'} & 0 & 0 & 0 & 0 & 0 & 0 & \psi_1^{'} & \psi_2^{'} & \psi_3^{'} \\ 0 & 0 & 0 & \psi_1^{'} & \psi_2^{'} & \psi_3^{'} & -\psi_1^{'} & -\psi_2^{'} & -\psi_3^{'} & 0 & 0 & 0 \\ 0 & 0 & 0 & \psi_1^{''} & \psi_2^{''} & \psi_3^{''} & -\psi_1^{''} & -\psi_2^{''} & -\psi_3^{''} & 0 & 0 & 0 \\ \psi_1^{''} & \psi_2^{''} & \psi_3^{''} & 0 & 0 & 0 & 0 & 0 & 0 & \psi_1^{''} & \psi_2^{''} & \psi_3^{''} \end{bmatrix}_{4\times 12}$$

$$\xi = \begin{bmatrix} 0 & GA & 0 & 0 \\ -GA & 0 & 0 & 0 \\ 0 & 0 & 0 & EI \\ 0 & 0 & -EI & 0 \end{bmatrix}_{4\times 4}$$